Atmospheric Correction Issues over Water

K. Stamnes, W. Li, H. Eide, K. Zhang, M. Ottaviani, and D. Cohen

Stevens Institute of Technology, Hoboken, NJ 07030

R. Spurr

RT Solutions, Inc., Cambridge, MA 02138

W. Wiscombe

NASA/Goddard Space Flight Center, Greenbelt, MD 20771

W. Su

NASA/Langley Research Center, Hampton, VA 23681

Outline

Part I:

- **Are Current Aerosol Models Adequate for Atmospheric Correction Purposes?**
- **How to Choose Aerosol Models?**
- **Possible Advantages offered by the Use of a "Continuum" Set of Models**

Part II:

- **How to Deal With Surface BRDF over Water?**
- **Are Existing Surface BRDF Models Adequate?**
- **Can We Design a Better Sunglint Mask?**
- **Can We Improve Sunglint Corrections?**

Light and Life Laboratory STEVENS Institute of Technology

Background/Motivation:
What Can be Done with Ocean Color Data?

Ocean color data can be used to remotely evaluate:

1. water quality;
2. transport of sediments and adhered pollutants;
3. primary production, upon which commercial fish populations depend for food;
4. harmful algal blooms that pose a threat to public health and economies of affected areas.

But reliable retrievals require:

- *accurate characterization of the atmosphere – a challenging problem over turbid coastal waters.*

Light and Life Laboratory STEVENS Institute of Technology

MODIS/SeaWiFS: Employs a "Discrete" Set of Aerosol Models

The MODIS ocean color group has adopted two basic aerosol models:

- **a *small particle "Tropospheric" (T) model* consisting of 70% water-soluble (e.g. ammonium, organic compounds, etc.) and 30% dust-like (e.g. clay, quartz, etc.) particles;**
- **a *large particle "Oceanic" (O) model* consisting of sea salt (e.g. sodium, potassium chloride, etc.) particles.**

A combination of these two small (T) and large (O) particle models yields:

- **a "Coastal" (C) aerosol model with 99.5% small and 0.5% large particles;**
- **a "Maritime" (M) aerosol model with 99% small and 1% large particles.**

This yields 4 aerosol models: 2 mono-modal and 2 bi-modal, but by allowing for 4 different relative humidities (50%, 70%, 90% and 99%) one arrives at a total of:

- **16 "discrete" MODIS aerosol models: T-50, ···, T-99; C-50, ···, C-99, M-50, ···, M-99; O-50, ···, O-99: half *mono-modal*, the other half *bi-modal*, whereas**
- **SeaWiFS employs a subset of 12 "discrete" aerosol models arranged in the following order from 1 through 12: O-90, O-99; M-50, M-70, M-90, M-99; C-50, C-70, C-90; T-50, T-90, T-99.**

Light and Life Laboratory STEVENS Institute of Technology

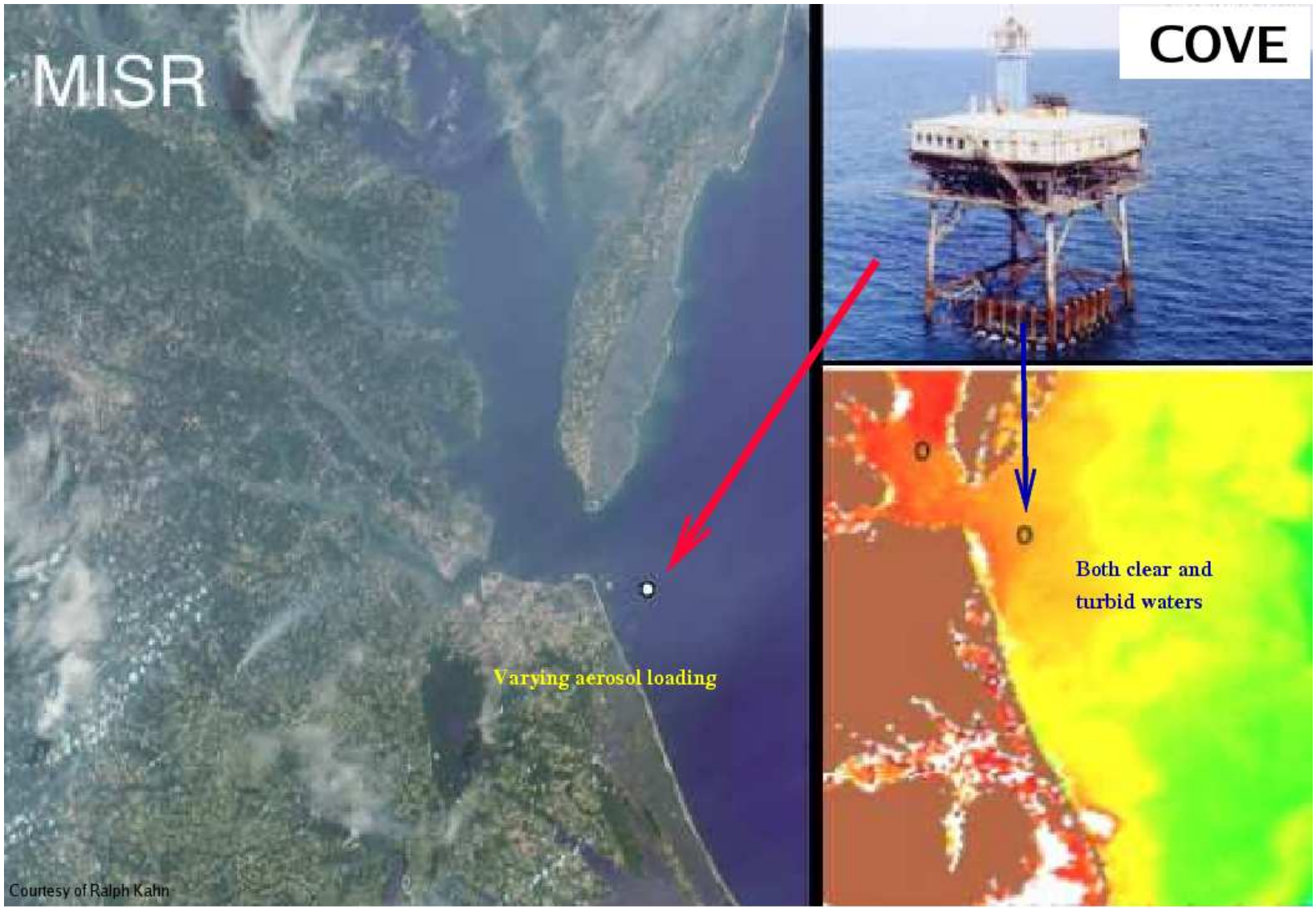

Figure 1: **The waters surrounding the COVE platform change between turbid and almost clear, and also the aerosol types and loading vary greatly at this site.** **Courtesy of Ken Rutledge NASA/Langley.**

Six Year SEAWIFS Archive Data

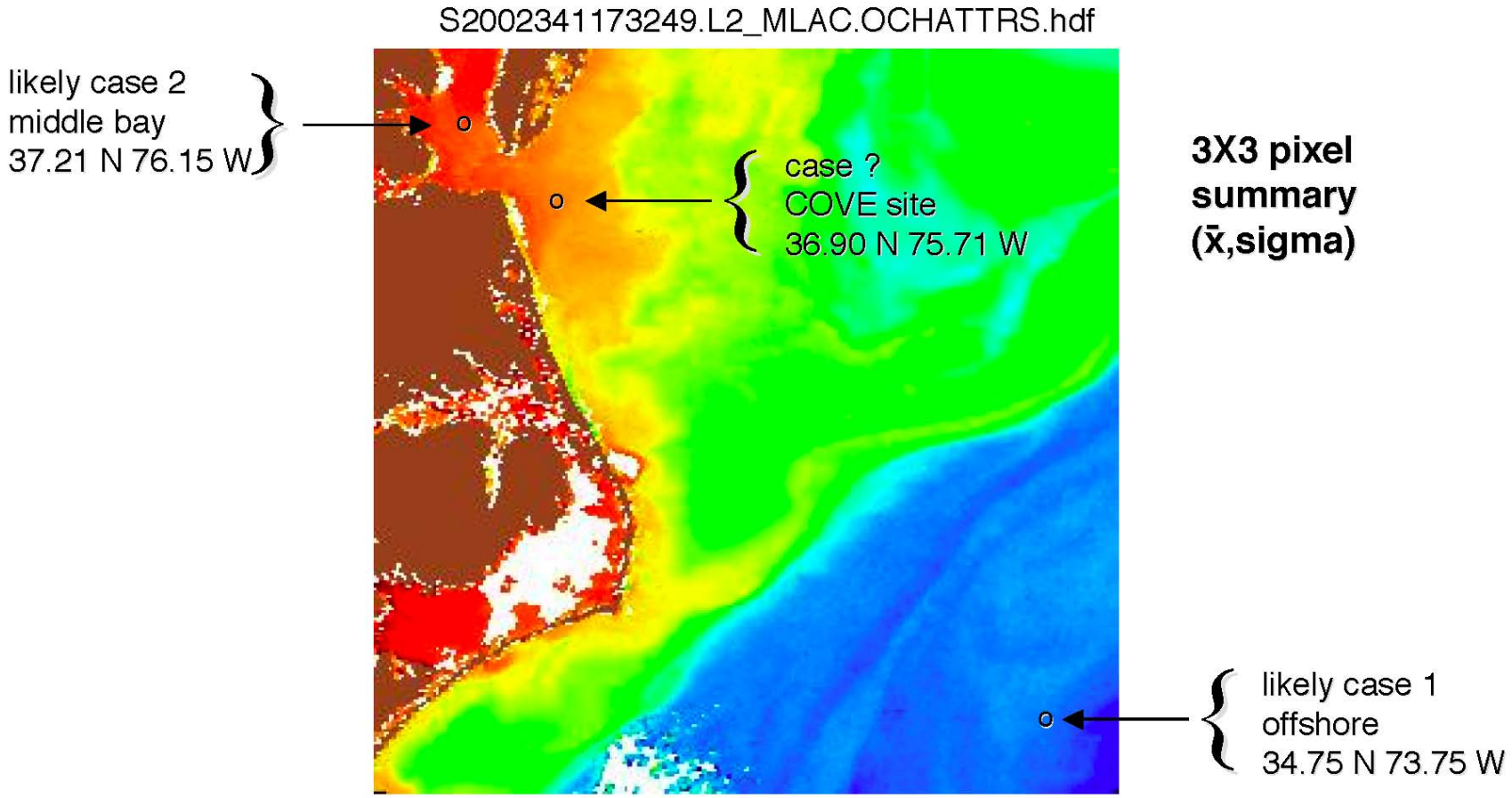

Figure 2: **Sample SEAWIFS-retrieved chlorophyll concentrations in clear and turbid waters.** Courtesy of Ken Rutledge NASA/Langley.

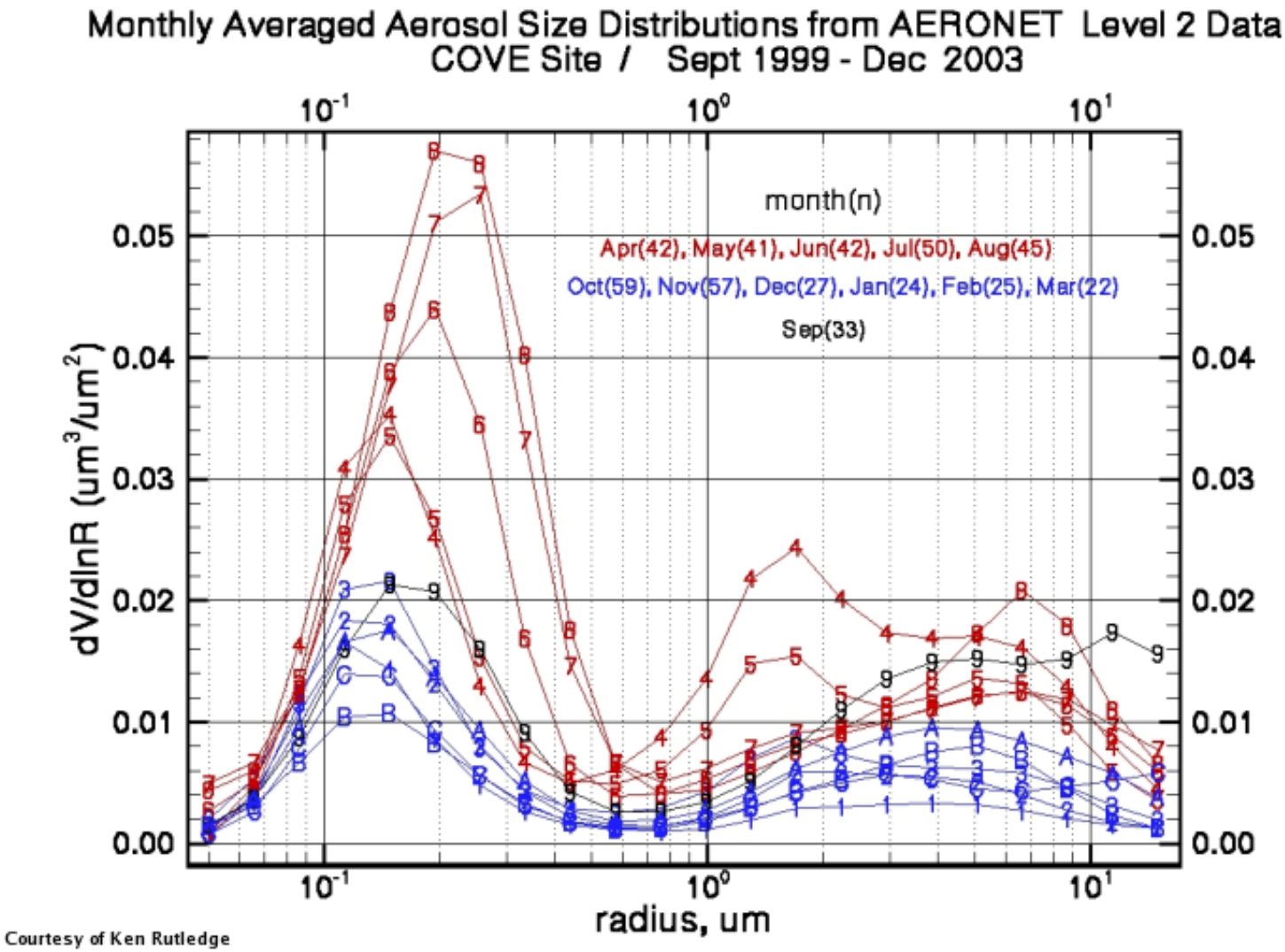

Figure 3: **Comparison of monthly means for the aerosol size distributions retrieved from surface observations of sky radiances by the AERONET sunphotometer on COVE.** Courtesy of Ken Rutledge NASA/Langley.

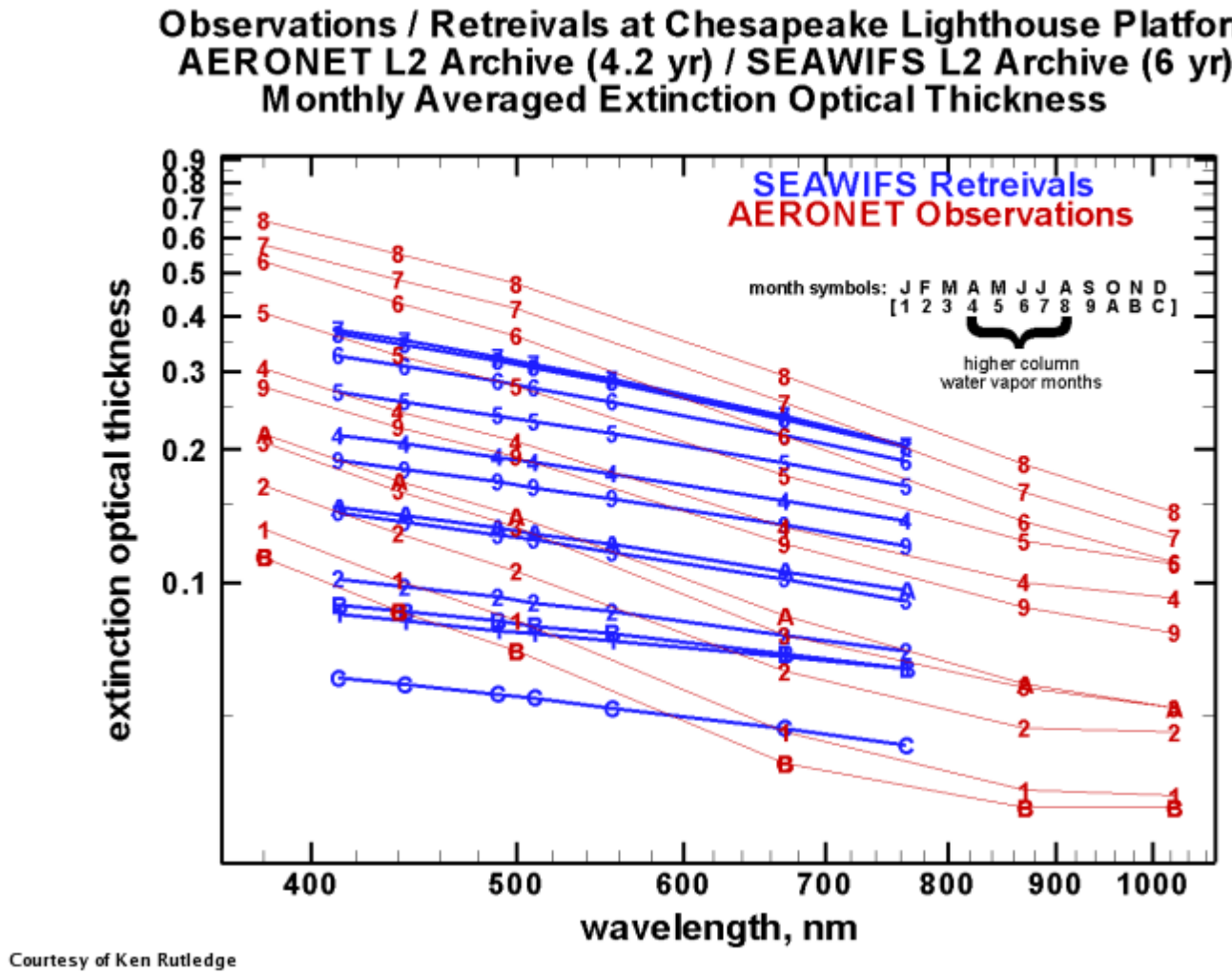

Figure 4: **Comparison of mean monthly optical thickness derived from surface observations (AERONET) and satellite retrievals (SeaWIFS) for a multi-year data-set obtained at the COVE site.** Courtesy of Ken Rutledge NASA/Langley.

We adopt: 16 Models Selected From a "Continuum" Set of Aerosol Models

We start with a combination of a small particle model and a large particle model:

- Small particle model: T-50 $\longleftarrow$ model #1 ($\eta = 0$ below).
- Large particle model: O-90 $\longleftarrow$ model #16 ($\eta = 1$ below).

Since the AERONET data seem to indicate that aerosol models are bi-modal in nature, we would like to construct a set of models such that most of them are bimodal. This can be done by using a linear combination of the two models:

- **Aerosol Model** $= (1-\eta)\times$ **T-50** $+ \eta\times$ **O-90**.
- **Then, picking the following values of η: 0, 0.0001, 0.0003, 0.0005, 0.0008, 0.0011, 0.0015, 0.002, 0.003, 0.004, 0.007, 0.01, 0.07, 0.225, 0.4575, 1:**
- **yields 16 discrete models selected from the continuum set obtained by letting η vary continuously between 0 and 1.**
- **The advantage of using this set instead the MODIS set is illustrated in the next two figures.**

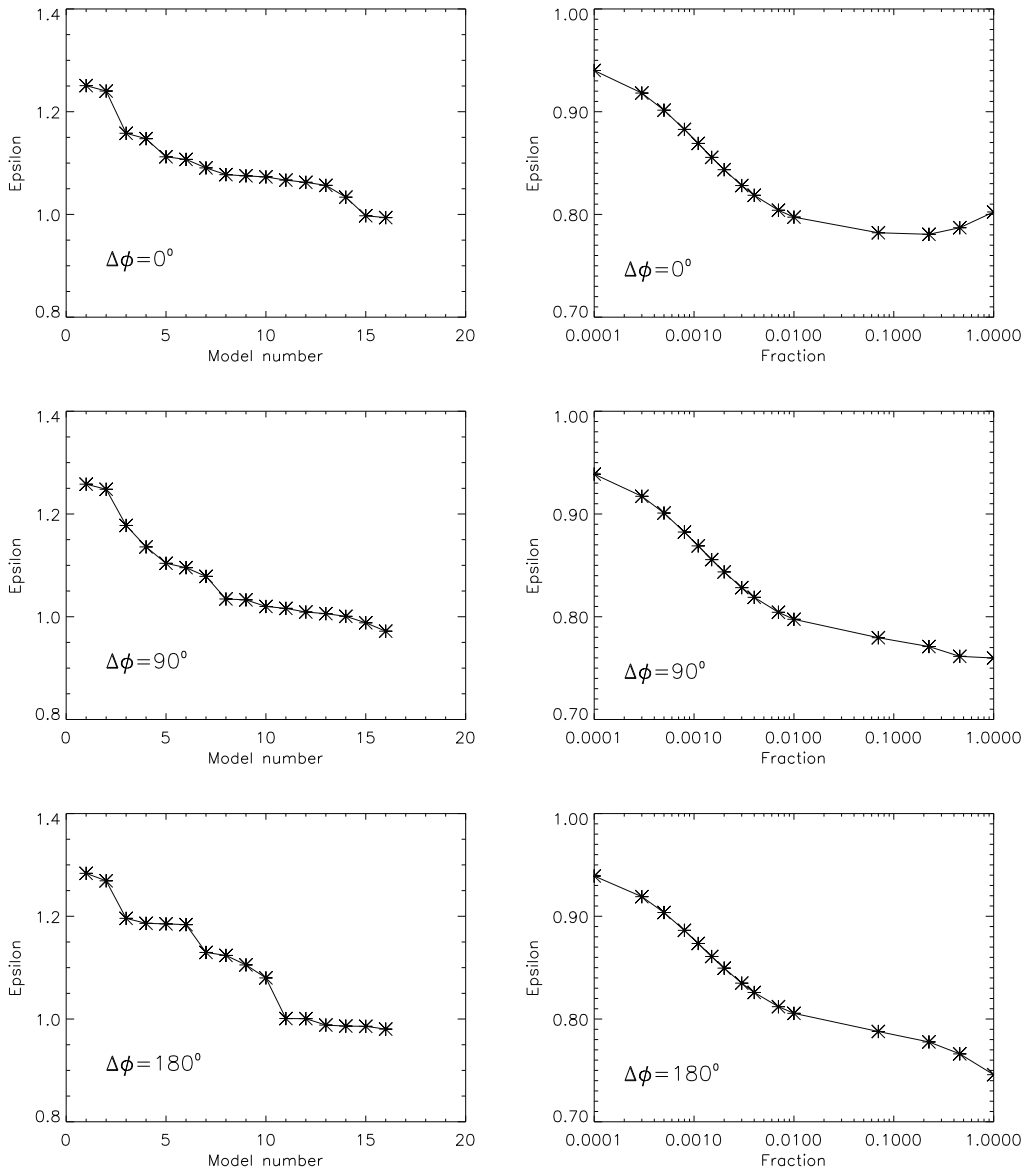

Figure 5: **Parameter $\epsilon_{ms}(765, 865) = [\rho_{atm}(765) - \rho_{ray}(765)]/[\rho_{atm}(865) - \rho_{ray}(865)]$ used for model selection. Left panel: *discrete* set of aerosol models. Right panel: *continuum* set of aerosol models. SZA = 45°, viewing angle = 30°.**

Extrapolation from the NIR into the Visible

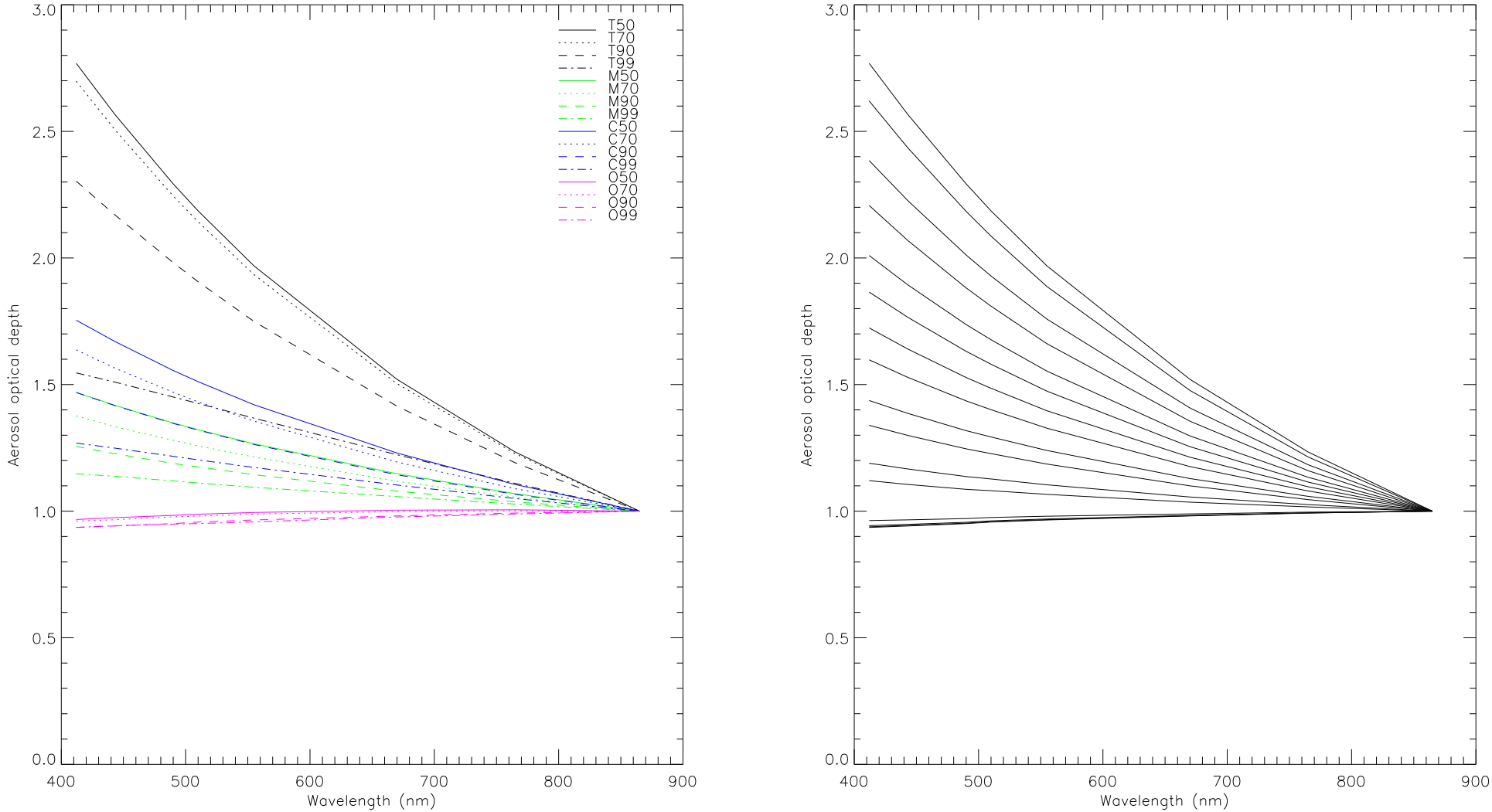

Figure 6: **Extrapolation of aerosol optical depth from the NIR into the visible. Left panel: *Discrete* MODIS aerosol models. Right panel: *Continuum* Models.**

Swedish Lakes: Simultaneous Retrieval of Aerosol Parameters, Chlorophyll Concentrations and Remote Sensing Reflectances

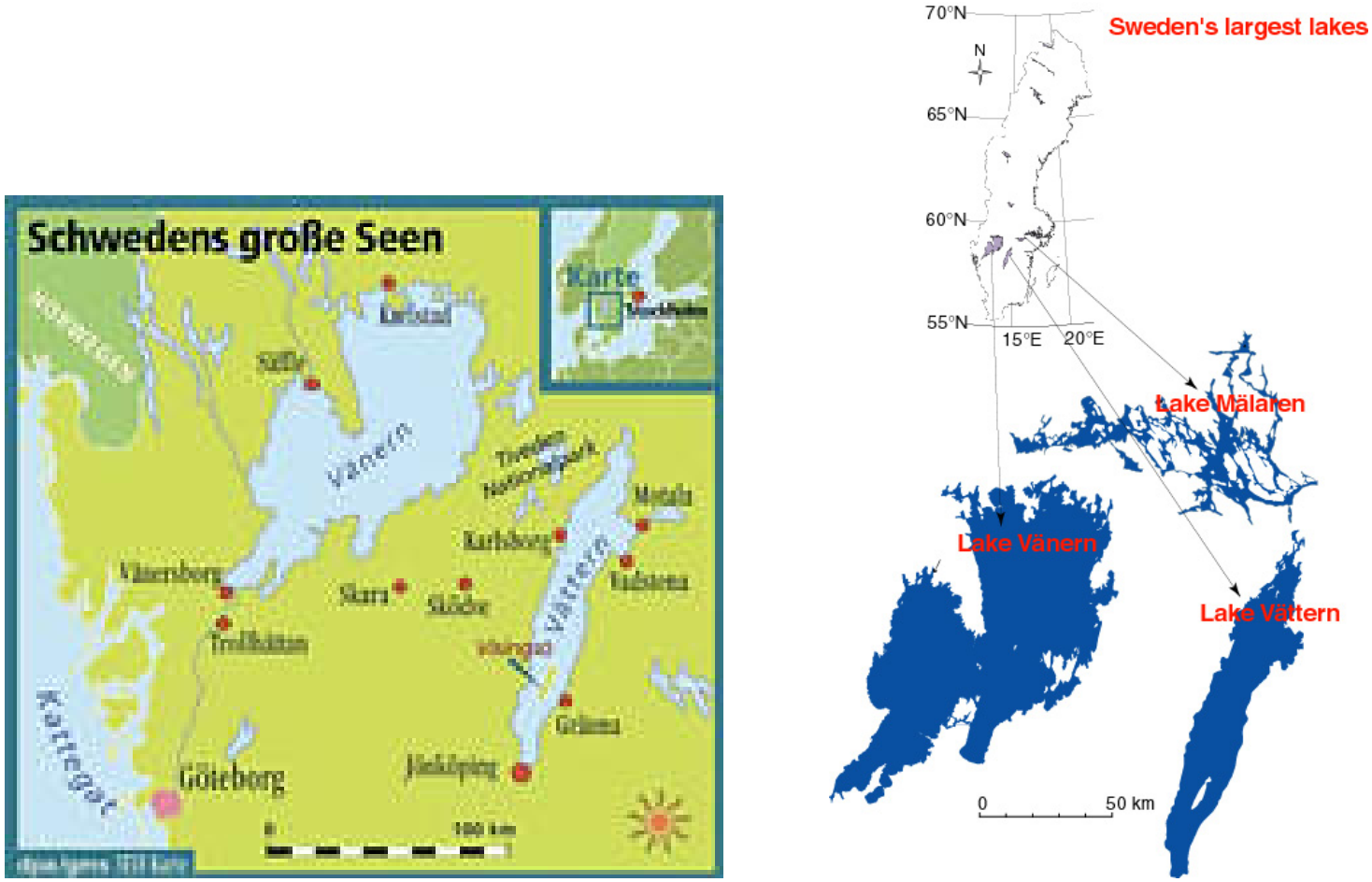

Figure 7: Map over area.

Left panel: CAO-DISORT. Right panel: SeaWiFS.

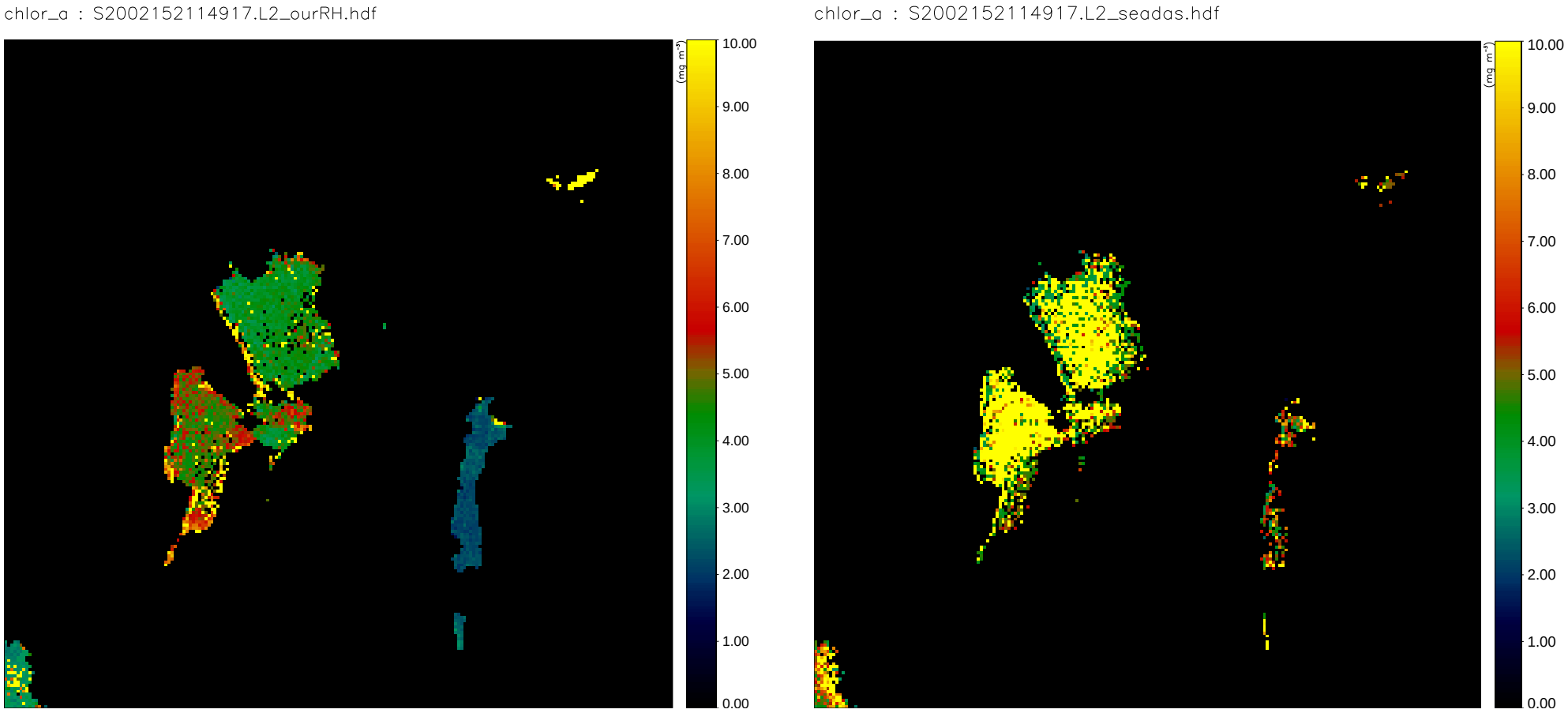

Figure 8: **Comparison of chlorophyll concentrations.**

Left panel: CAO-DISORT. Right panel: SeaWiFS.

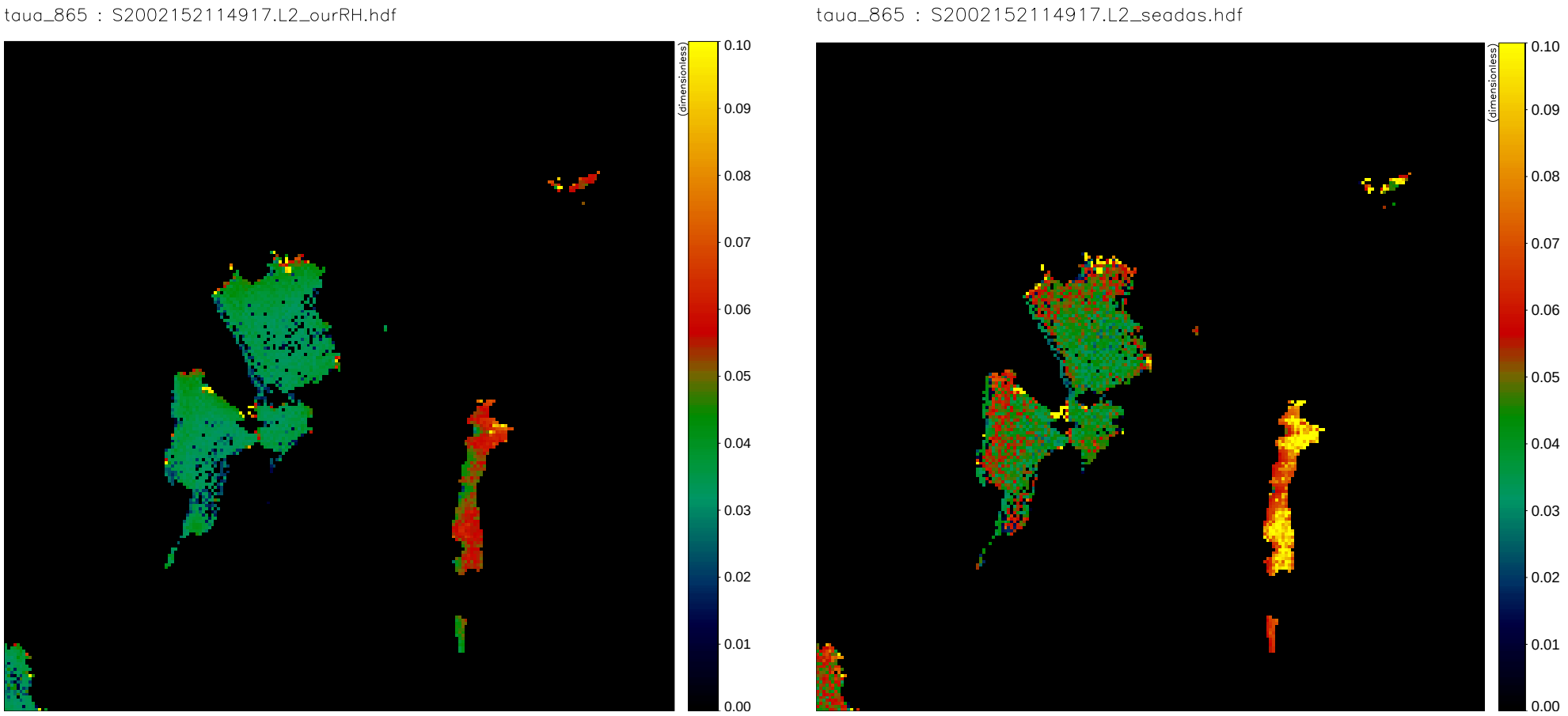

Figure 9: **Comparison of aerosol optical depths at 865 nm.**

Left panel: CAO-DISORT. Right panel: SeaWiFS.

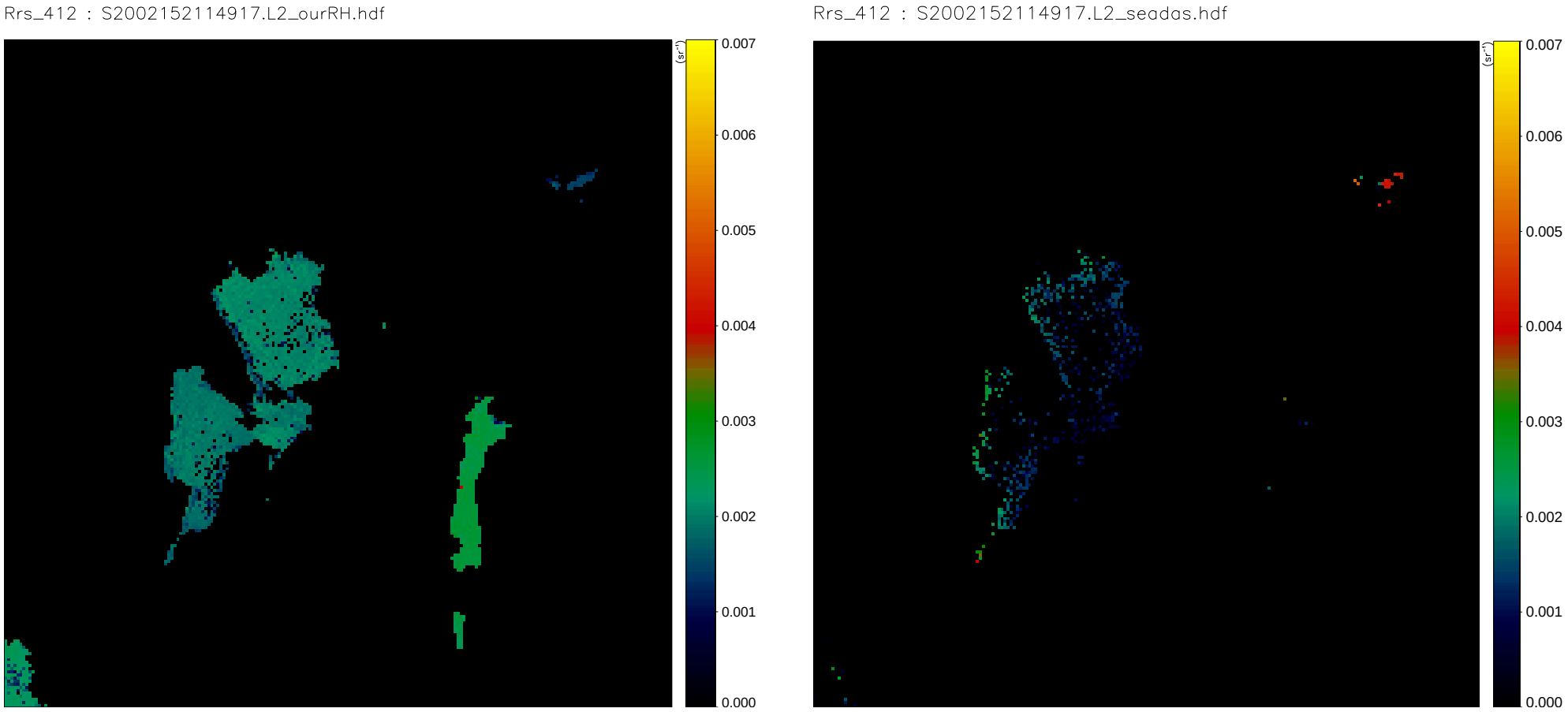

Figure 10: **Comparison of retrieved remote sensing reflectances at 412 nm.**

Left panel: CAO-DISORT. Right panel: SeaWiFS.

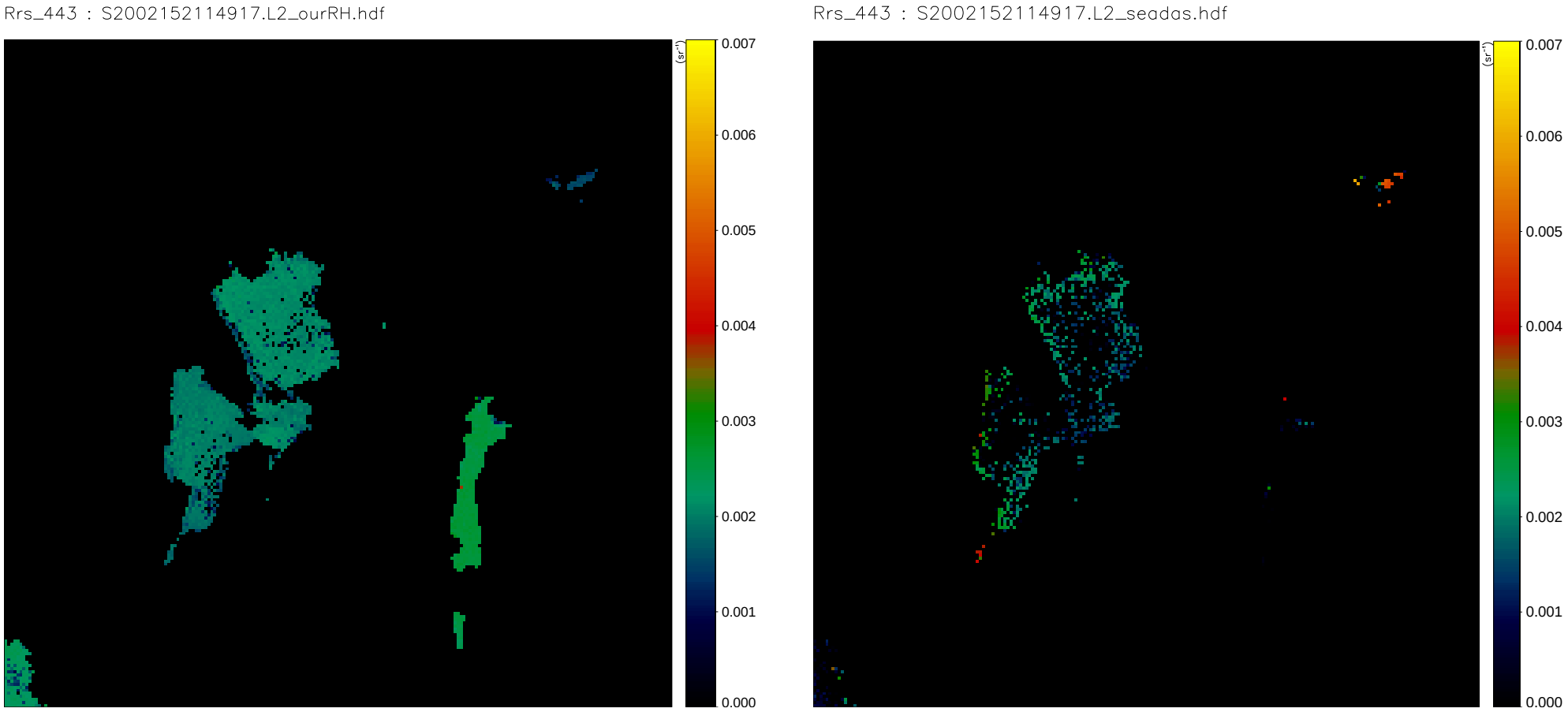

Figure 11: **Comparison of retrieved remote sensing reflectances at 443 nm.**

Left panel: CAO-DISORT. Right panel: SeaWiFS.

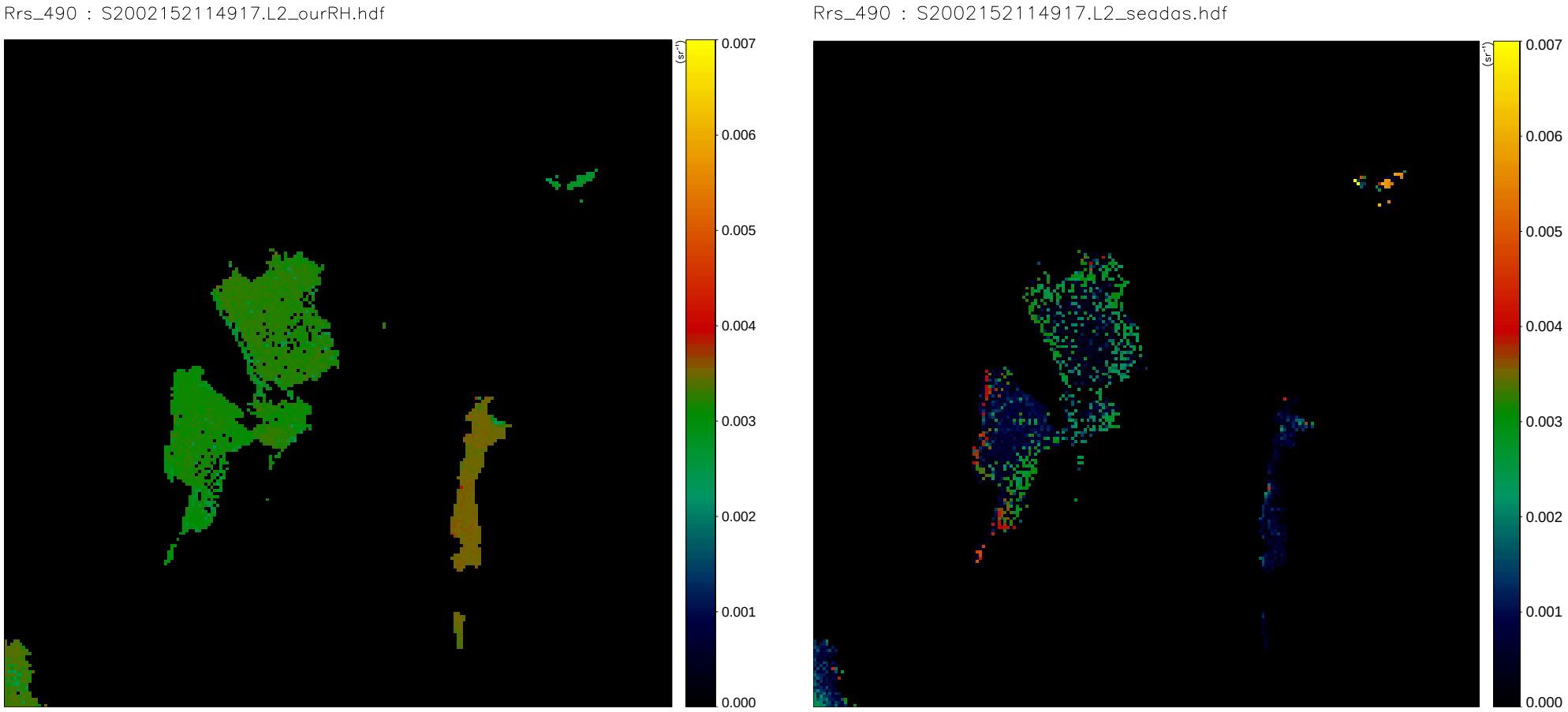

Figure 12: **Comparison of retrieved remote sensing reflectances at 490 nm.**

Left panel: CAO-DISORT. Right panel: SeaWiFS.

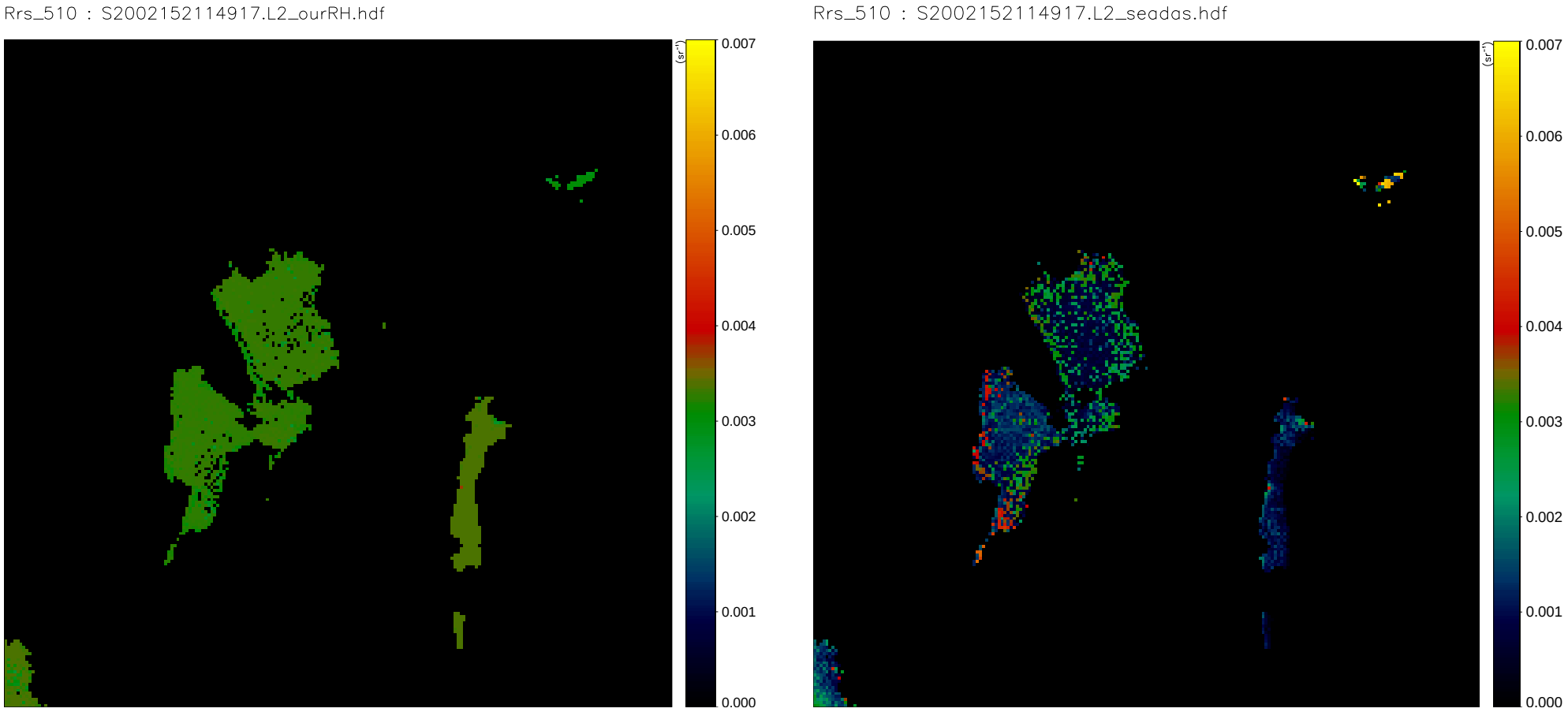

Figure 13: **Comparison of retrieved remote sensing reflectances at 510 nm.**

Left panel: CAO-DISORT. Right panel: SeaWiFS.

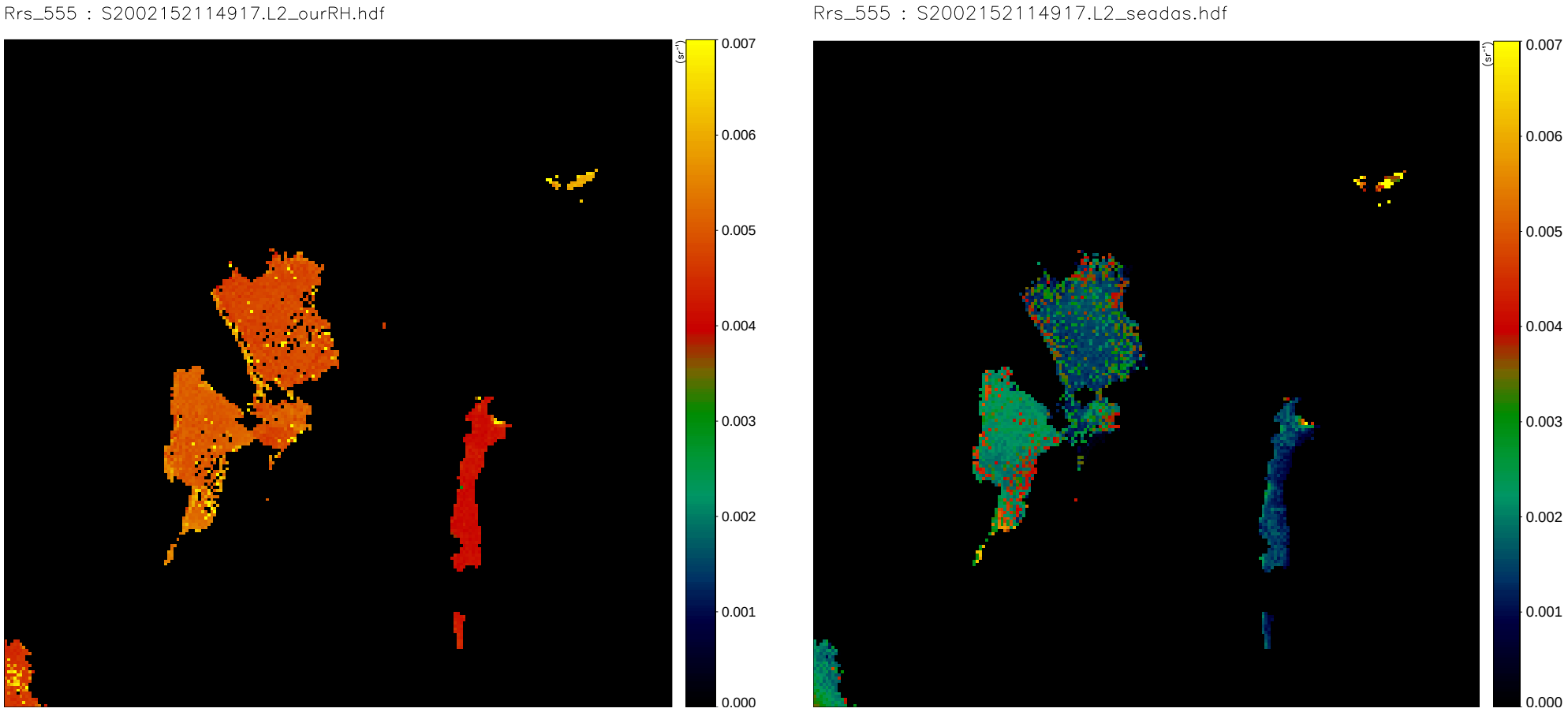

Figure 14: **Comparison of retrieved remote sensing reflectances at 555 nm.**

Left panel: 412 nm. Right panel: 443.

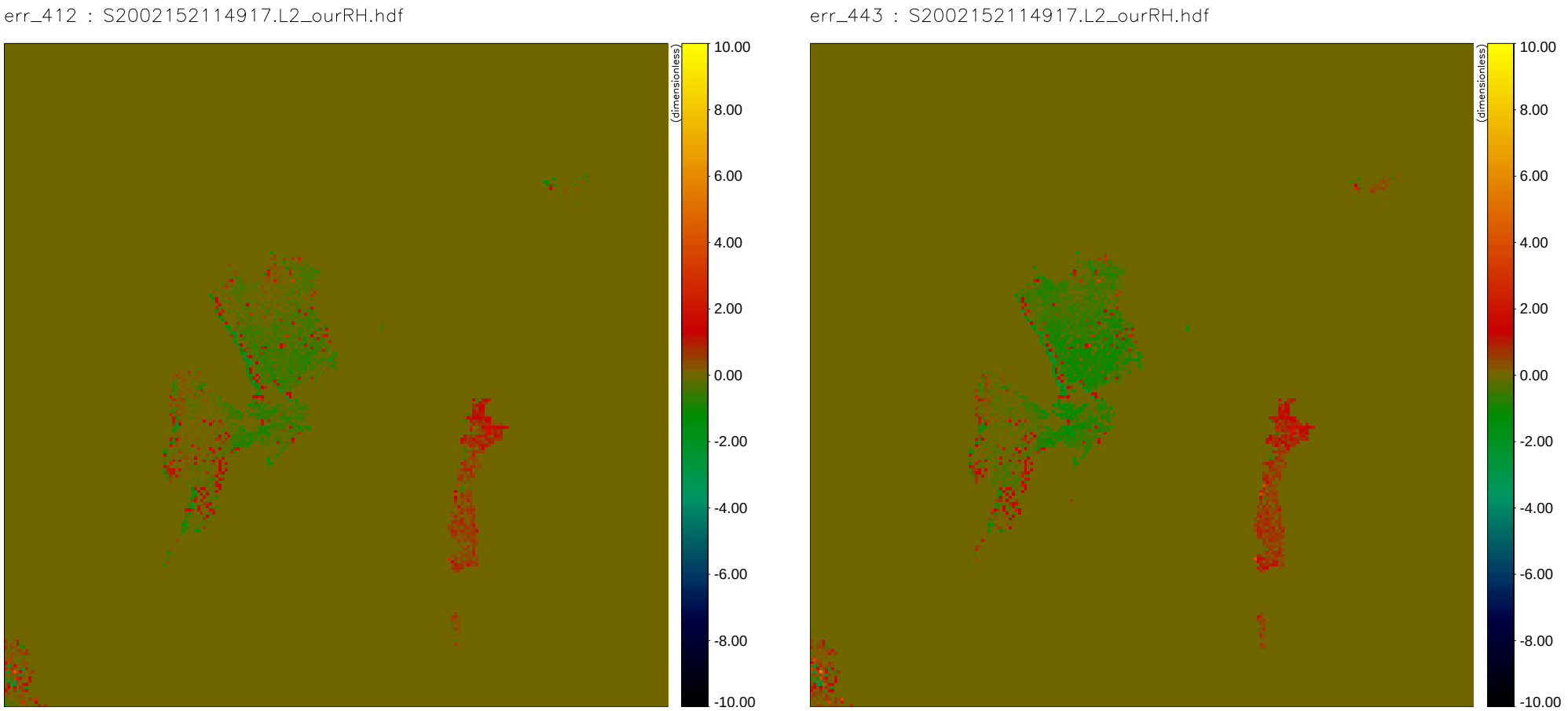

Figure 15: **Percentage Error in the TOA Reflectances Computed as:** $\{[\rho_{meas} - t\rho_w - \rho_{path})]/\rho_{meas}\} \times 100$.

Left panel: 490 nm. Right panel: 510.

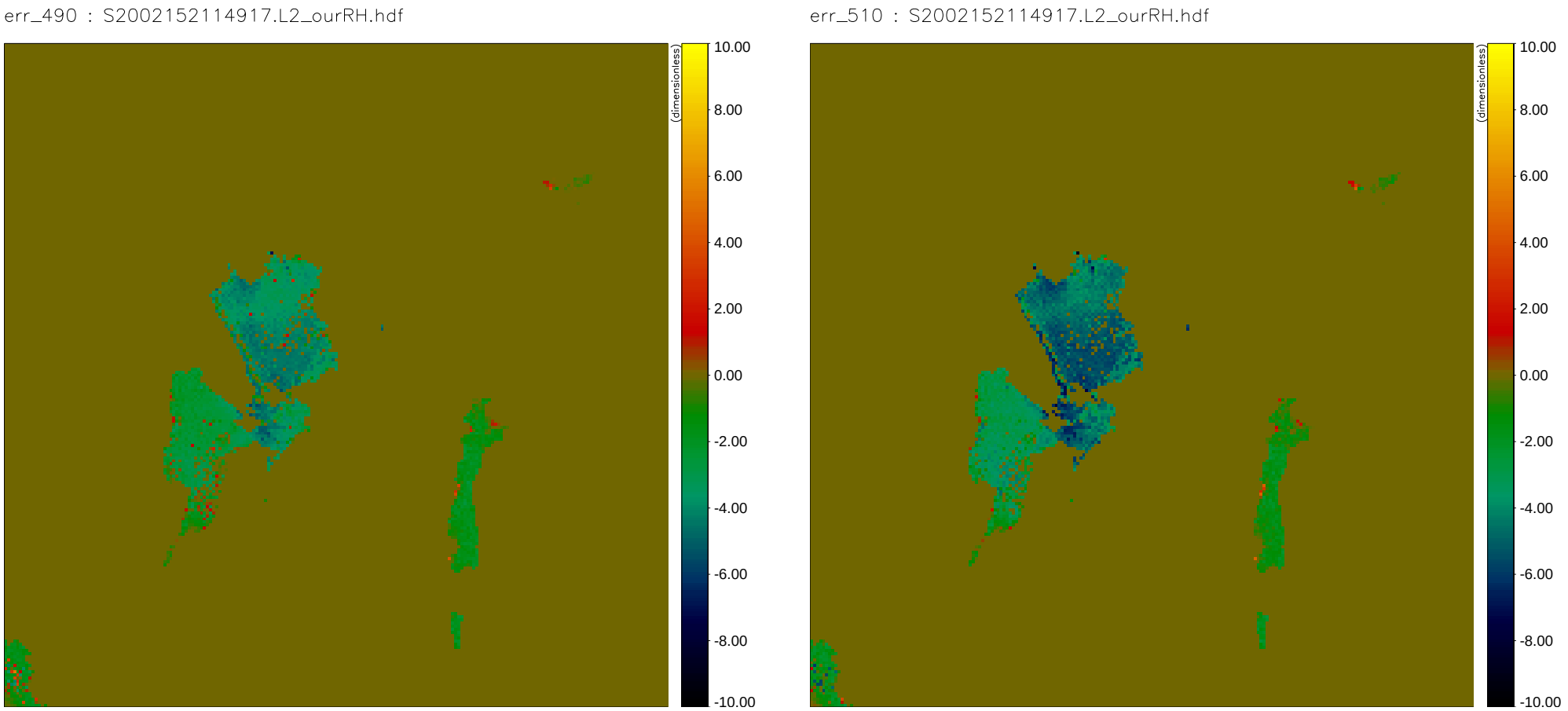

Figure 16: **Percentage Error in the TOA Reflectances Computed as:** $\{[\rho_{meas} - t\rho_w - \rho_{path})]/\rho_{meas}\} \times 100$.

Left panel: 555 nm. Right panel: 670.

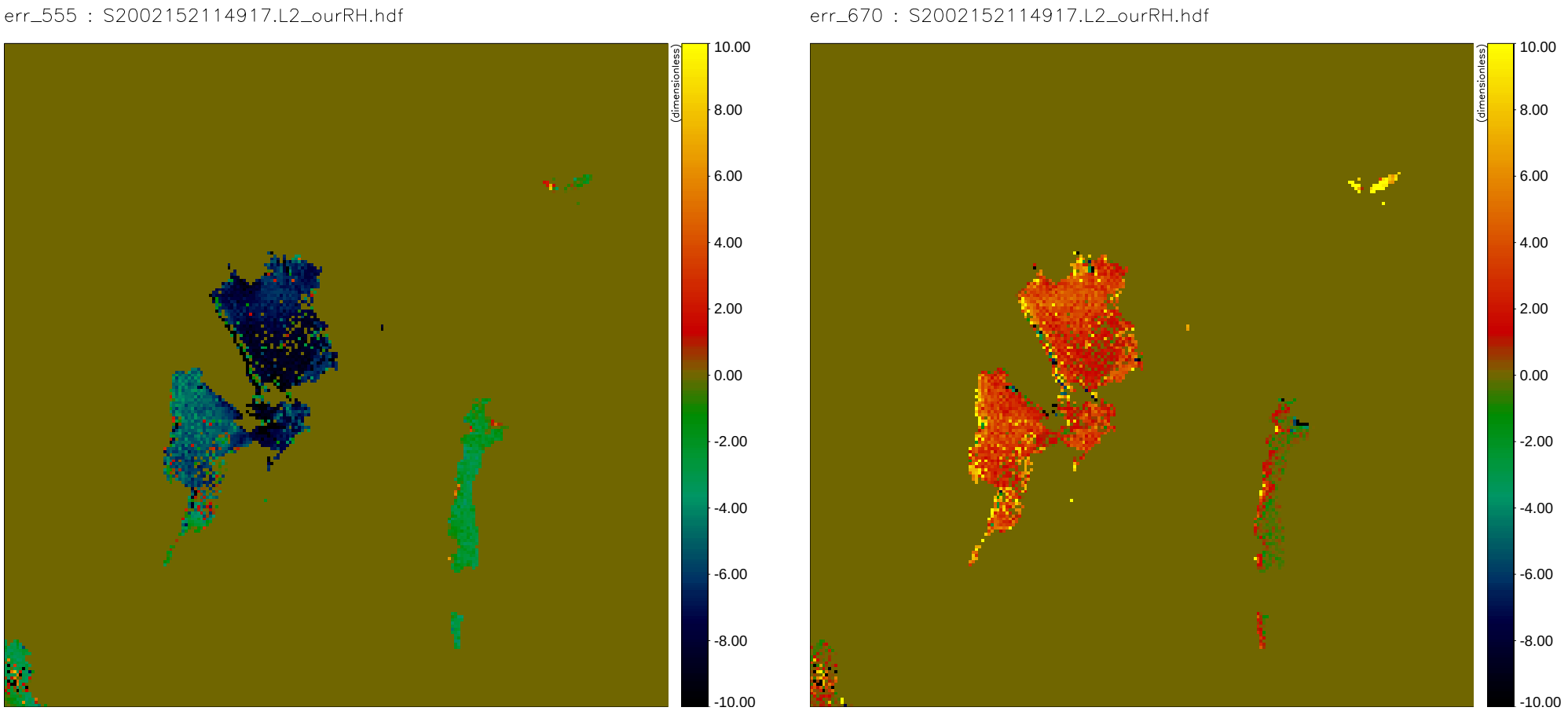

Figure 17: **Percentage Error in the TOA Reflectances Computed as:** $\{[\rho_{meas} - t\rho_w - \rho_{path})]/\rho_{meas}\} \times 100$.

Left panel: 765 nm. Right panel: 865.

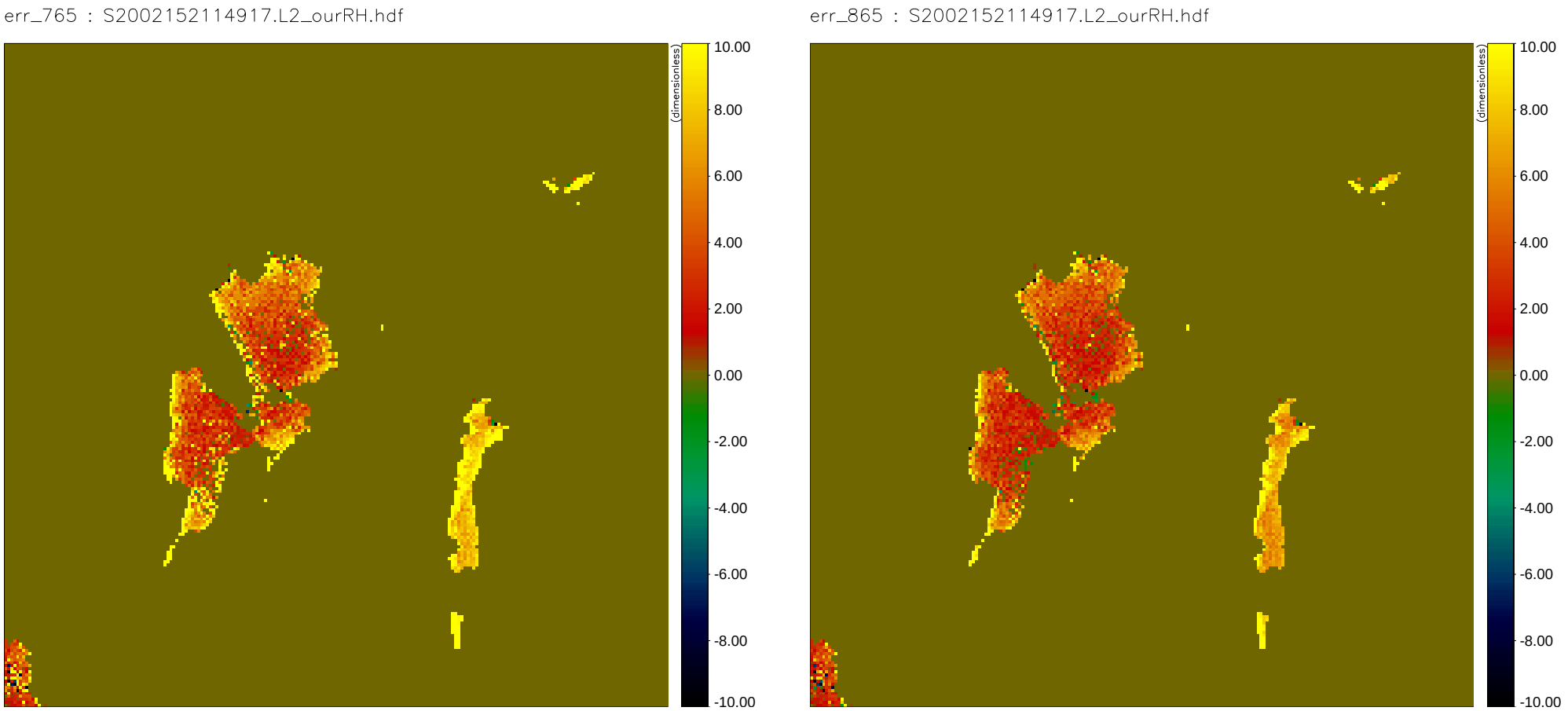

Figure 18: **Percentage Error in the TOA Reflectances Computed as:** $\{[\rho_{meas} - t\rho_w - \rho_{path})]/\rho_{meas}\} \times 100$.

Summary – Part I

We may summarize the previous figures as follows:

- The SeaWiFS algorithm performs rather poorly for this particular image, and yields lots of negative remote sensing reflectances (water-leaving radiances).
- By contrast, our simultaneous retrieval CAO-DISORT algorithm performs much better, and yields reasonable error budgets.
- Because our bio-optical model applies to ocean rather than lake water (Stamnes et al., 2003), and the aerosol models are generic rather than site-specific, we find these results encouraging.
- We conjecture that the CAO-DISORT algorithm could produce better results with a lake-specific bio-optical model, and with local information about aerosol properties.

Reference:

Stamnes, K., W. Li, B. Yan, H. Eide, A. Barnard, W. S. Pegau and J. J. Stamnes, Accurate and self-consistent ocean color algorithm: simultaneous retrieval of aerosol optical properties and chlorophyll concentrations, Appl. Opt., 42, 939-951, 2003.

PART II: Air-Water Interface $\cdots$ *Surface Waves* (1)

The questions are:

- Can we construct a reliable sunglint mask that can be used to screen for sunglint?
- Given a reliable sunglint mask: To what extent is it possible to correct for sunglint in ocean color imagery?
- Can a better understanding/description of sunglint be used to our advantage?

There are two important issues to consider:

1. What is the correct sunglint BRDF of a real (wavy) ocean surface?
2. Given the correct sunglint BRDF: What is the corresponding TOA radiance?

The first issue relates to:

- our understanding/knowledge of **surface roughness** due to winds, currents, etc. whereas the second one is related to
- **atmospheric radiative transfer.**

Air-Water Interface $\cdots$ *Surface Waves (2)*

How do we treat sunglint? The Cox/Munk Model:

Cox/Munk expressed the slope distribution by a Gram-Charlier series:

$$P(z'_x, z'_y) = \frac{e^{-\frac{\xi^2+\eta^2}{2}}}{2\pi\sigma'_x\sigma'_y}\{1 - \frac{1}{2}C_{21}(\xi^2-1) - \frac{1}{6}C_{03}(\eta^3-3\eta) \tag{1}$$
$$+ \frac{1}{24}C_{40}(\xi^4-6\xi^2+3) + \frac{1}{4}C_{22}(\xi^2-1)(\eta^2-1) + \frac{1}{24}C_{04}(\eta^4-6\eta^2+3)\}$$

where
$\xi = z'_x/\sigma'_x$, $\eta = z'_y/\sigma'_y$
σ'_x and σ'_y are rms values of z'_x and z'_y
C_{21} and C_{03} are **skewness** coefficients
C_{40}, C_{22} and C_{04} are **peakedness** coefficients.

Here (WS = wind speed):

$$\begin{aligned} \sigma_x'^2 &= 0.003 + 0.00192\ \mathrm{WS} \pm 0.002 \qquad \sigma_y'^2 = 0.00316\ \mathrm{WS} \pm 0.004 \\ C_{21} &= 0.01 - 0.0086\ \mathrm{WS} \pm 0.03 \qquad C_{03} = 0.004 - 0.033\ \mathrm{WS} \pm 0.12 \\ C_{40} &= 0.40 \pm 0.23 \qquad C_{22} = 0.12 \pm 0.06 \qquad C_{04} = 0.23 \pm 0.41. \end{aligned} \tag{2}$$

Air-Water Interface $\cdots$ *Surface Waves* (3)

How do we treat sunglint? The Cox/Munk Model (continued):

Note that in the absence of skewness ($C_{21} = C_{03} = 0$), and peakedness ($C_{40} = C_{22} = C_{04} = 0$) the Gram-Charlier series reduces to a 2-D Gaussian:

$$P(z'_x, z'_y) = \frac{e^{-\frac{\xi^2+\eta^2}{2}}}{2\pi\sigma'_x\sigma'_y}.$$

Furthermore, if $\sigma'_x = \sigma'_y = \sigma' \Longrightarrow z'_x = z'_y = z'$, then we obtain a 1-D Gaussian:

$$P(z') = \frac{e^{-\frac{\xi^2+\eta^2}{2}}}{2\pi\sigma'^2}.$$

Air-Water Interface $\cdots$ *Surface Waves* (4)

How do we treat sunglint? The Cox/Munk Model (continued):

The sunglint reflectance is then written as (ignoring shadowing and multiple reflections):

$$\rho_{glint}(\theta_s, \theta_v, \Delta\phi) = \frac{\pi P(z'_x, z'_y)\rho_F(n_w, \theta_s, \theta_v, \Delta\phi)}{4\cos(\theta_s)\cos(\theta_v)\cos^4(\beta)}$$

where $\rho_F(n_w, \theta_s, \theta_v, \Delta\phi)$ is the Fresnel reflection coefficient, and n_w the index of refraction of water.

How do we compute the Fresnel reflection coefficient $\rho_F(n_w, \theta_s, \theta_v, \Delta\phi)$?

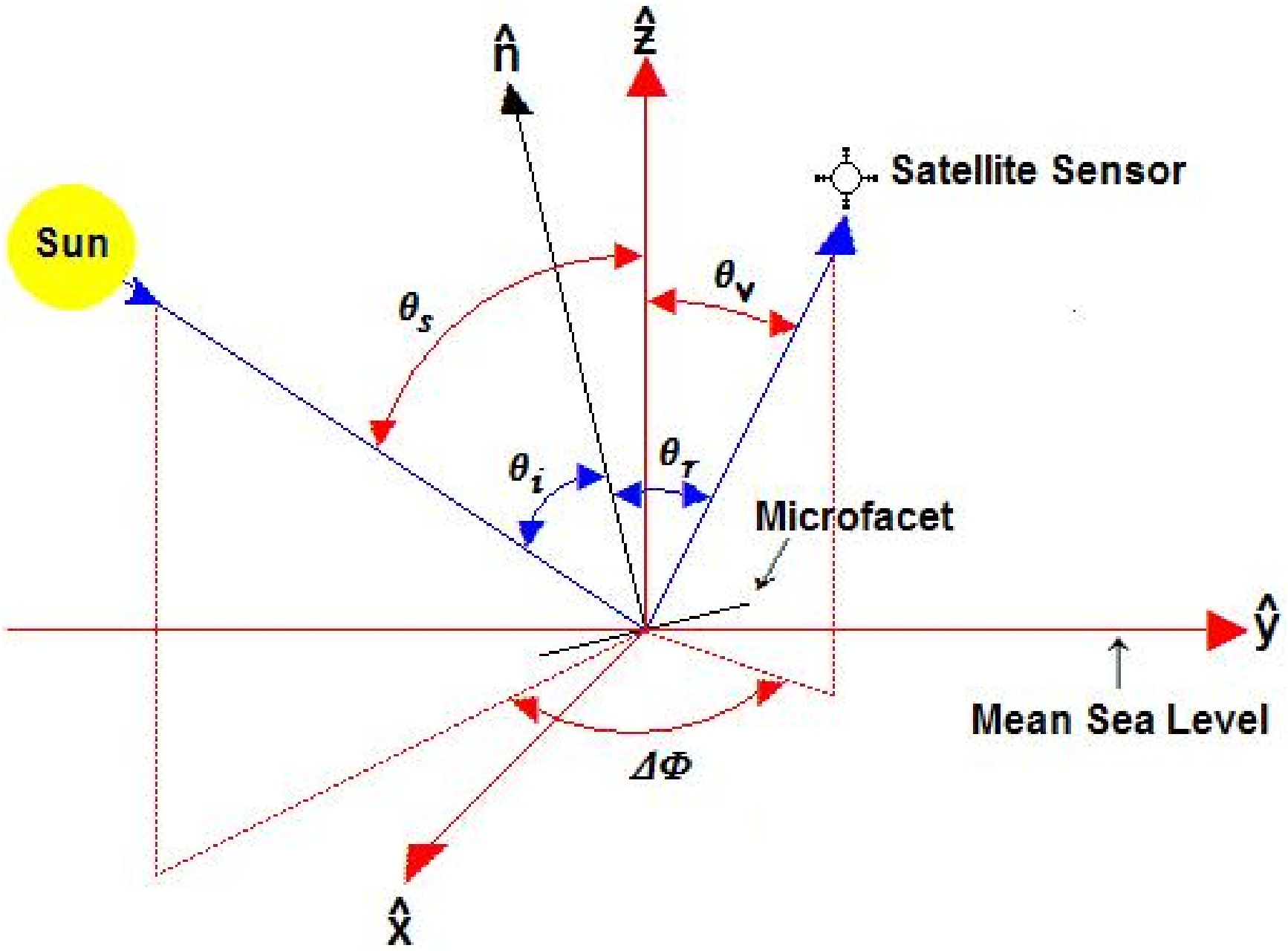

Figure 19: **The Sun-satellite Geometry, and Definition of Angles.**

Air-Water Interface $\cdots$ *Surface Waves* (5)

For unpolarized incident light, the flux reflectance and transmittance become:

$$\rho_F = \frac{1}{2}(\rho_{TE}^2 + \rho_{TM}^2) \qquad \mathcal{T}_F = \frac{1}{2}(\mathcal{T}_{TE}^2 + \mathcal{T}_{TM}^2)$$

where the subscripts "TE" and "TM" refer to the electric vector perpendicular (TE wave) and parallel (TM wave) to the plane of incidence, respectively.

These formulas apply to any of the plane micro-facets that make up the wavy ocean surface $\Longrightarrow$ **we need to relate the angle of incidence θ_i on an individual microfacet to the angles $\theta_s, \theta_v, \Delta\phi = \phi_s - \phi_v$ that describe the sun-satellite geometry w.r.t. a flat surface.**

Using spherical trigonometry, we find:

$$\cos\theta_i = \sqrt{\frac{1}{2}[1 + \cos(\theta_s)\cos(\theta_v) + \sin(\theta_s)\sin(\theta_v)\cos\Delta\phi]}$$

$$\sin\theta_i = \sqrt{\frac{1}{2}[1 - \cos(\theta_s)\cos(\theta_v) + \sin(\theta_s)\sin(\theta_v)\cos\Delta\phi]}.$$

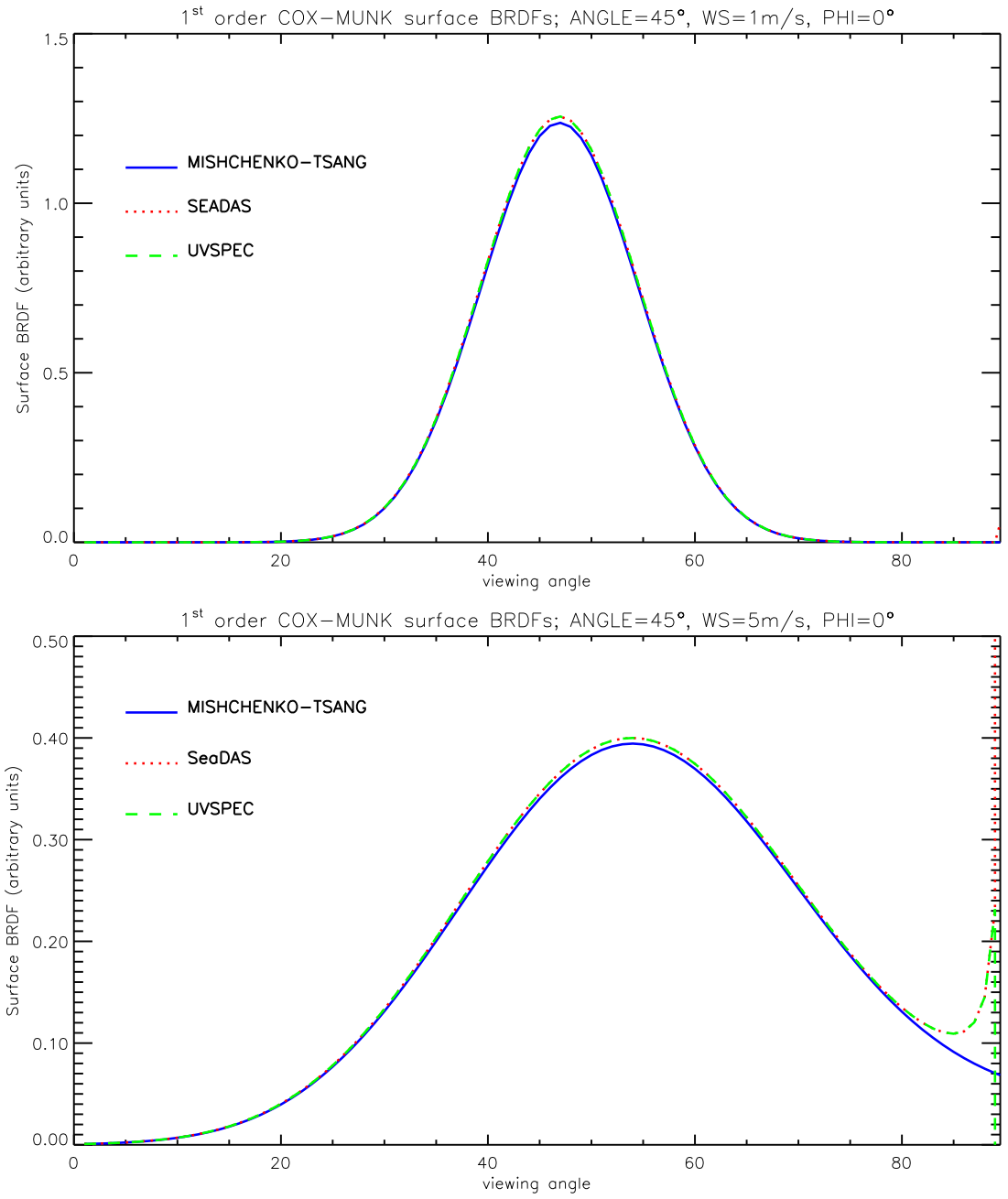

Figure 20: **Comparison of BRDF computed with 3 different codes.**

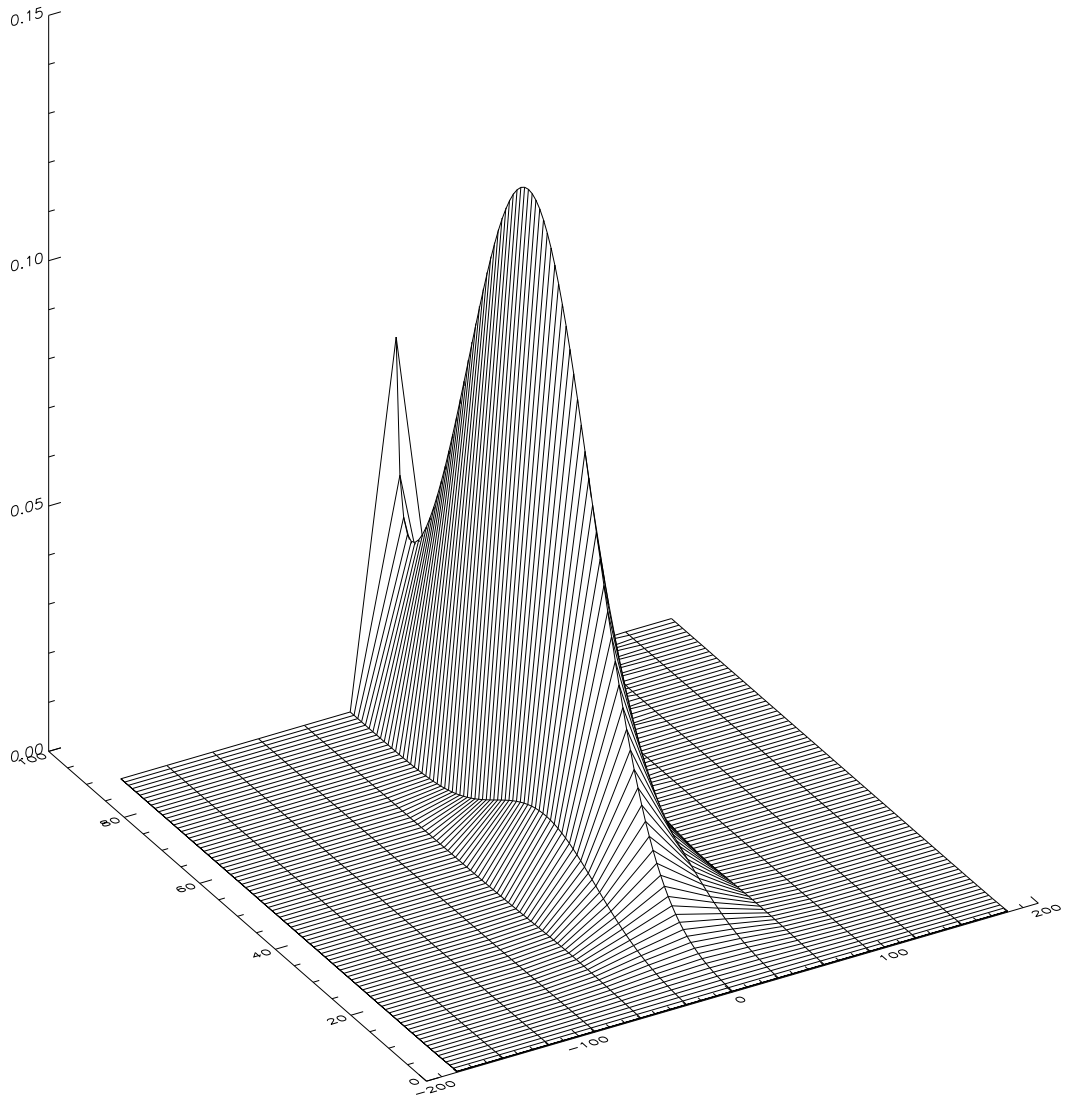

Figure 21: **3-D display of the BRDF.**

Air-Water Interface $\cdots$ *Surface Waves* (6)

The remaining question is: Given the sunglint BRDF, $\rho_{glint}(\theta_s, \theta_v, \Delta\phi)$, what is the corresponding TOA radiance?

The **direct** sunglint TOA radiance is (F^s = incident TOA irradiance):

$$L_{TOA}(\theta_s, \theta_v, \Delta\phi) = \rho_{glint}(\theta_s, \theta_v, \Delta\phi)\frac{\mu_s F^s}{\pi} e^{-\tau(\frac{1}{\mu_s}+\frac{1}{\mu_v})} \qquad \tau = \tau_R + \tau_A$$

θ_s = solar zenith angle; $\mu_s = \cos\theta_s$;
θ_v = polar viewing angle; $\mu_v = \cos\theta_v$;
τ_R = optical depth due to Rayleigh scattering;
τ_A = optical depth due to aerosol absorption and scattering.

Note that the **direct** sunglint approach:

- **ignores multiple scattering and thus the contribution from "skyglint" to the TOA radiance.**

Air-Water Interface $\cdots$ *Surface Waves* (7)

To properly take into account the contribution from the surface we must solve the radiative transfer equation:

$$\mu\frac{dL(\tau,\mu_v,\phi_v)}{d\tau} = L(\tau,\mu_v,\phi_v) - \overbrace{\frac{1}{4\pi}\int_0^{2\pi}d\phi'\int_0^1 d\mu p(\tau,\mu',\phi';\mu_v,\phi_v)L(\tau,\mu',\phi')}^{multiple\ scattering} - \overbrace{\frac{F^s}{4\pi}p(\tau,-\mu_s,\phi_s;\mu_v,\phi_v)e^{-\tau/\mu_s}}^{single\ scattering}$$

subject to the boundary condition:

$$L(\tau=\tau_a,\mu_v,\phi_v) = \overbrace{\frac{1}{\pi}\mu_s F^s e^{-\tau_a/\mu_s}\rho_{glint}(-\mu_s,\phi_s;\mu_v,\phi_v)}^{direct\ sunglint} + \overbrace{\frac{1}{\pi}\int_0^{2\pi}d\phi'\int_0^1 d\mu'\mu'\rho_{glint}(-\mu',\phi';\mu_v,\phi_v)L(\tau_a,-\mu',\phi')}^{skyglint}. \quad (3)$$

Air-Water Interface $\cdots$ *Surface Waves* (8)

The effect of multiple scattering can be obtained by using a RT code such as DISORT (ftp://climate1.gsfc.nasa.gov/wiscombe/), as implemented in UVSPEC (http://libradtran.org), which allows for the inclusion of a BRDF.

To compute the total glint contribution to the TOA radiance, we may:

- compute the **total** TOA radiance, $L_{TOA}^{tot}(\theta_v, \theta_s, \Delta\phi)$, using Eq. (3) as the lower boundary condition;
- compute the TOA radiance, $L_{TOA}^{bsurf}(\theta_s, \theta_v, \Delta\phi)$, for a black surface by setting $\rho_{glint} = 0$ in Eq. (3);
- compute the total (direct + diffuse) glint contribution to the TOA radiance as:

$$L_{TOA}^{glint}(\theta_s, \theta_v, \Delta\phi) = L_{TOA}^{tot}(\theta_s, \theta_v, \Delta\phi) - L_{TOA}^{bsurf}(\theta_s, \theta_v, \Delta\phi).$$

In this way, we obtain **the total "glint" contribution**, because we have:

- **included multiply scattered** sky radiation **reflected** from the surface, but **ignored** sky radiation ***not*** **reflected** from the surface.

Air-Water Interface $\cdots$ *Surface Waves* (9)

What is the difference between the *direct glint radiance* (used in SeaDAS) and the *total glint radiance* obtained by including multiple scattering?

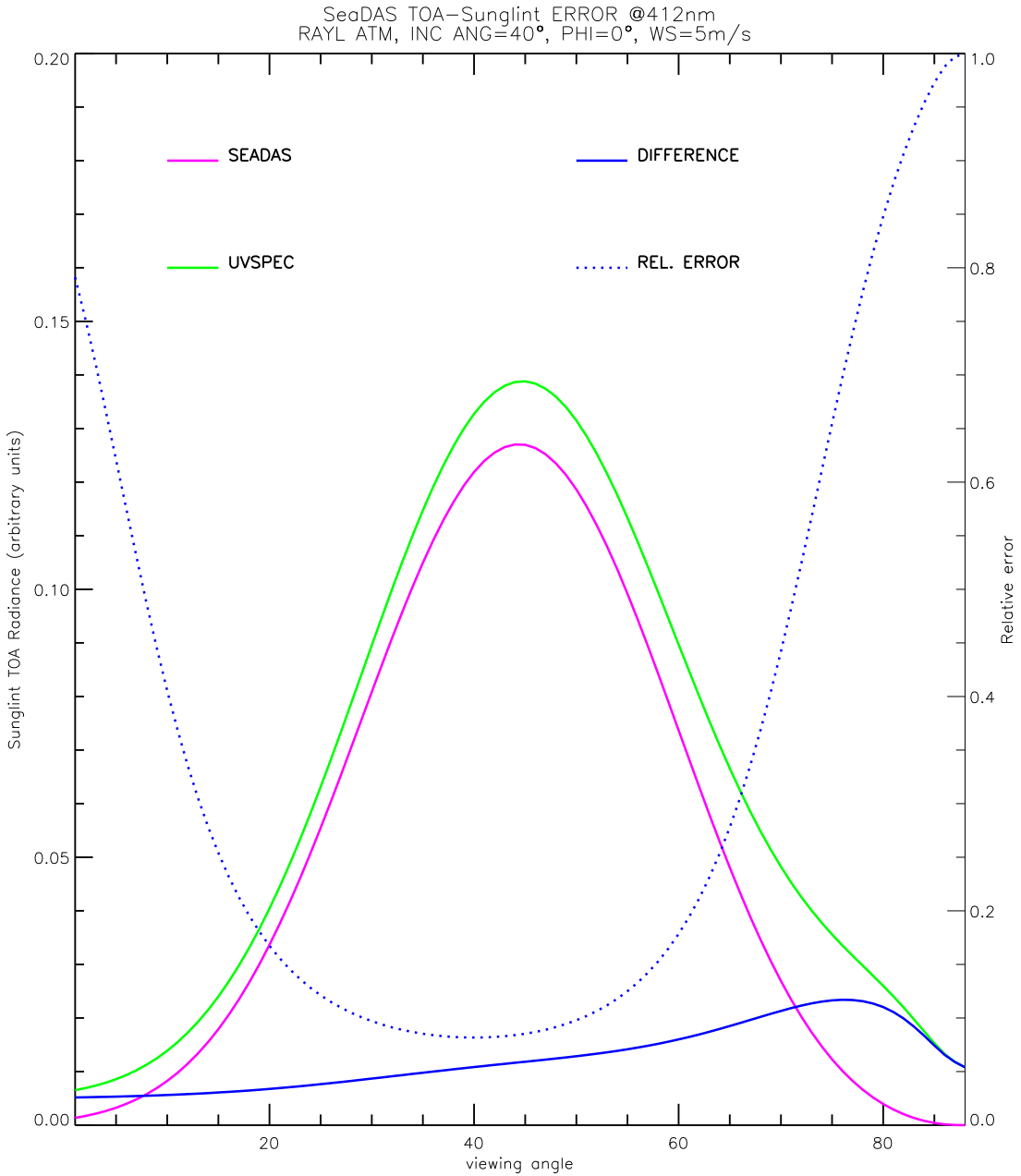

Figure 22: **Comparison of TOA radiances *in the principal plane* at 412 nm for a Rayleigh atmosphere.**

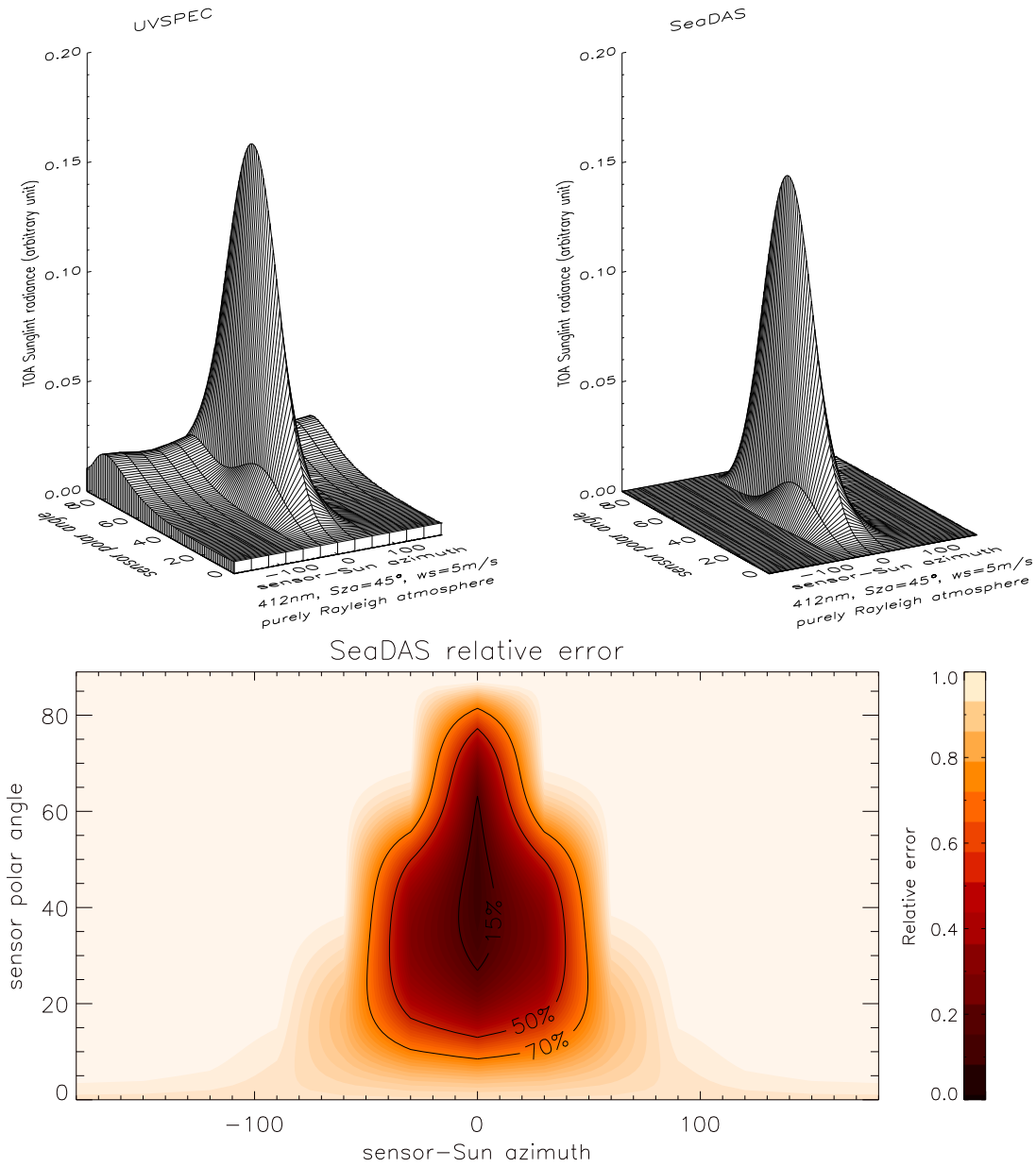

Figure 23: **Comparison of 3-D TOA radiances at 412 nm.**

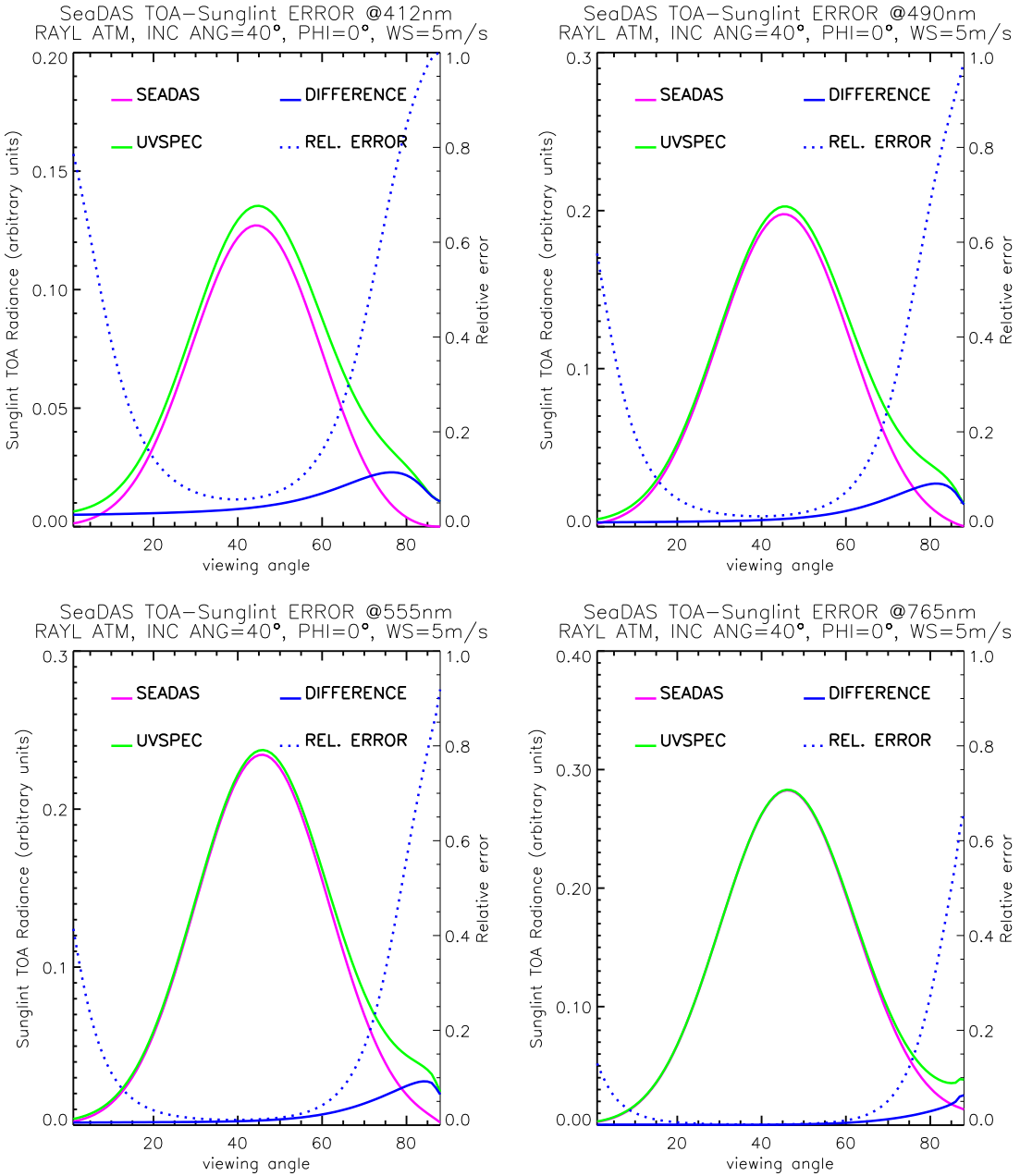

Figure 24: **Comparison of TOA glint radiances *in the principal plane* at four different wavelenghts for a Rayleigh atmosphere.**

Summary – Part II

For a given sunglint BRDF it is possible to:

1. compute accurate TOA radiances for **unpolarized** light that can be used to construct a reliable sunglint mask, and thereby:
2. extend the region of sunglint corrected imagery by including the effect of multiple scattering on the TOA radiance.

Remaining questions include:

- Is the Cox/Munk distribution of slopes presently used for surface BRDF adequate?
- What measurements are needed to improve the situation?
- Can we use polarization to improve our treatment of scattering effects?
- Can we use sunglint as a "known" source at the surface to help us retrieve atmospheric properties and thereby improve "atmospheric correction" of ocean color imagery?

Light and Life Laboratory STEVENS Institute of Technology

Figure 25: **“Mirror” reflection of sunlight off calm water.**

Figure 26: **“Mirror” reflection of sunlight off calm water.**

Figure 27: **"Mirror" reflection of sunlight off calm water.**

Figure 28: **"Sunglint": reflection of sunlight off "ruffled" water.**

Figure 29: **“Sunglint”: reflection of sunlight off “ruffled” water.**